Aquacultural Engineering 54 (2013) 64–71

Contents lists available at SciVerse ScienceDirect

Aquacultural Engineering

journal homepage: www.elsevier.com/locate/aqua-online

Digital image analysis as a tool to quantify gaping and morphology in smoked salmon slices

Grigory V. Merkin[a,*], Lars Helge Stien[b], Karin Pittman[a], Ragnar Nortvedt[a,c]

[a] Department of Biology, University of Bergen, High Technology Centre, N-5020, Bergen, Norway
[b] Institute of Marine Research, Austevoll Research Station, 5392 Storebø, Norway
[c] MedViz, Haukeland University Hospital, 5021 Bergen

ARTICLE INFO

Article history:
Received 23 January 2012
Accepted 15 November 2012

Keywords:
Image analysis
Image segmentation
Smoked salmon
Gaping
Slice quality
Slice shape

ABSTRACT

Gaping in salmon fillets refers to the appearance of slits in the muscle. This is unsightly and leads to downgrading and hence economical loss, particularly for salmon smoke houses. Present day manual and semi automatic methods for quantifying gaping are labour intensive and subjective. This study presents an automated and objective image analysis method for quantifying gaping in smoked salmon slices. The slices are first photographed in a photobox and then analysed by the fully automated image analysis method. The method has four main steps: (1) pre-processing, (2) segmentation of slices from the background, (3) labelling of each slice, (4) identification of gaps within the slices (holes), (5) identification of gaps on the perifery (notches) and (6) quantification of gaps and notches. The results obtained by the automatic image analysis are visually convincing and there is a strong correlation with manual quantification of gaps ($r = 0.83$, p-value < 0.05). The automatic image analysis method can easily be extended to also include morphological parameters as shape, red and white muscle area, myocommata and myotome area. Interestingly, the automatic image analysis demonstrated that gaps are strongly associated with white, and not red, muscle tissue.

1. Introduction

Intrinsic characteristics such as colour, texture (the physical feel of the substance), gaping (appearance of slits in the axial muscle) and chemical composition are important for salmon fillet quality (Rasmussen, 2001). During processing the evaluation of salmon fillet quality is performed on the level of raw fillets (Andersen et al., 1994; Ashton et al., 2010; Roth et al., 2009), smoked fillets (Birkeland et al., 2004) and smoked fillet slices (Bernardi et al., 2009; Espe et al., 2004a).

In whole salmon fillets gaping appears as slits, whereas in smoked salmon slices gaping appears as holes in the slices (gaps) and notches into the slice borders. The estimation of gaping is typically done by visually grading fillets or fillet slices, either by counting gaps according to the "Andersen scale" (Andersen et al., 1994) or by evaluating the area covered by gaps (Kiessling et al., 2004). These methods rely on manual assessment by trained evaluators using standardised methodology. Consequently, the significant disadvantages of available approaches for gaping evaluation is that they are both labour demanding and subjective (Lavety et al., 1988; Robb, 2001). There is therefore a need for automated and objective methods for assessing gaping in salmon flesh.

Automated image analysis is a modern and efficient approach for monitoring quality traits in salmonids such as colour (Misimi et al., 2007; Quevedo et al., 2010; Stien et al., 2006), fat content (Stien et al., 2007), amount of red and white muscle (Stien et al., 2006), myocommata and myotome positions (Stien et al., 2006, 2007) and shape (Stien et al., 2006). The evaluation of gaping by using digital photography and computer image analysis can provide accurate and re-analysable data (Ashton et al., 2010). Recently Balaban et al. (2011) developed a semi-automatic method for analysing gaping in salmon fillets using a manually set threshold (Gonzalez and Woods, 2008) for each individual fillet image, where pixels on the fillet surface darker than the selected threshold are classified as gaping. As recognised by the authors, the recently proposed method for gaping evaluation will inherently lead to a certain bias in the threshold determination (threshold to produce two levels (binary) images from grayscale images (Glasbey and Horgan, 1995), as well as error when other dark parts on the fillet surface, such as melanin spots and bruises are mistakenly classified as gaping (Balaban et al., 2011).

Gaping is often concealed in salmon fillets and difficult to spot without handling the fillet (Michie, 2001) or disposing fillets skin-down over a surface with convex curvature (Ashton et al., 2010). Meanwhile, these hidden gaps are clearly revealed as gaps and

* Corresponding author. Tel.: +47 94276189.
E-mail address: Grigory.Merkin@bio.uib.no (G.V. Merkin).

0144-8609/$ – see front matter © 2012 Elsevier B.V. All rights reserved.
http://dx.doi.org/10.1016/j.aquaeng.2012.11.003

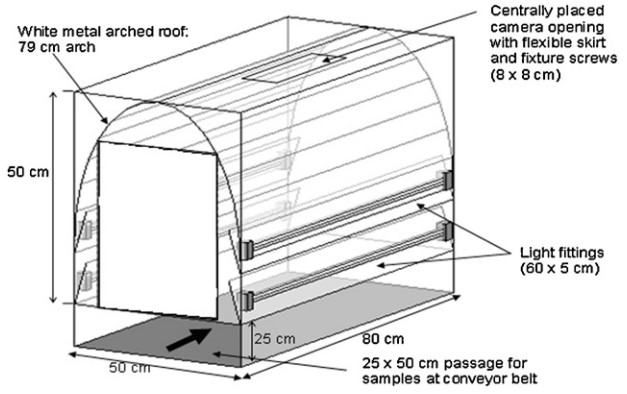

Fig. 1. Photobox (SeaSide AS).

notches once the fillet is sliced. The gaps penetrate the slices exposing the background under the respective slice (Fig. 2). The main aim of this article is to present a fully automatic image analysis method for quantifying gaping in smoked salmon slices. The results from applying this method on a set of slices are compared with results from manual segmentation using the mouse. In addition to investigating gaping in relation to slice morphology, we further developed the image analysis to also include other important quality characteristics as shape, amount of red and white muscle, white stripe (myocommata) and myotome area.

2. Materials and methods

2.1. Sample selection

Market size Atlantic salmon (*Salmo salar* L.) ($n = 135$) were sampled in September 2010 from Nofima Marine research station at Averøy on the West coast of Norway and transported on ice for one week, before machine filleting at Marine Harvest Kritsen fish processing factory (Marine Harvest®, France). After filleting and trimming the right fillet from each fish was weighted. The fillets had a mean (SD) weight of 1.3 (0.2) kg. The remaining left fillets were smoked overnight, machine sliced and packed with 4 slices in each package. A total of 77 packages were then randomly selected and opened.

2.2. Image aquisition

Fillet slices from every package were carefully placed on a horizontal white styrofoam base in a photobox (Fig. 1, SeaSide AS) and photographed directly from above with a digital camera (Basler A102fc®) using the following selected parameters (Exposure time (raw) 1000, red balance ratio 131, black level 0, gain 192, diaphragm 11). The photobox provided uniform and diffuse lighting on the scene in order to avoid reflexes (white areas which effectively remove information from that part of the scene) on the moist and shiny salmon slices and to avoid shadows inside the holes and notches obscuring the white background. The photobox also ensured that the lighting was identical from image to image ($T = 6500$ K, Ra ≥ 90). The output from the camera was RGB colour images (Glasbey and Horgan, 1995; Gonzalez and Woods, 2008). Each pixel (x, y) in an RGB colour image is a triplet corresponding to the intensity of the primary colours (R)ed, (G)reen, and (B)lue at that point (Glasbey and Horgan, 1995; Gonzalez and Woods, 2008). All captured RGB images were stored as files in bit map format (bmp) with a resolution of 1388×1038 pixels (Fig. 2). An object of known size demonstrated that an image area of 28×28 pixels corresponded to 1 cm^2.

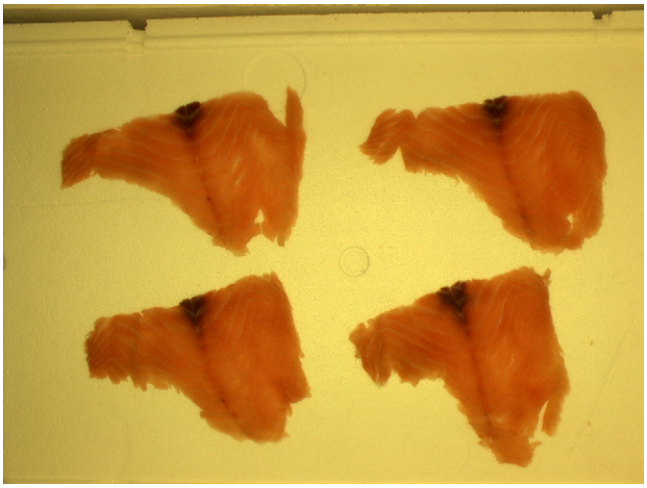

Fig. 2. Example of one of the original RGB images of smoked salmon slices.

2.3. Automatic image analysis method for gaping evaluation

The image analysis method was developed in Matlab (Version 7.10.0499 (R2010a), 32-bit (win 32), The Math-Works Inc., MA, USA) using the MATLAB® Image Processing Toolbox. The methodology is however standard and can be implemented in the many advanced image analysis software or programming languages. The method has six main steps (Fig. 3): (1) pre-processing (Fig. 4), (2) segmentation of slices from the background (Fig. 5) (3) Labelling of each slice, (4) identification and quantification of gaps (holes) inside the given slice region (Fig. 6) and (5) identification of gaps in the border of the slices (notches) (Fig. 7) and (6) quantification of gaps and notches. The operations were performed in the G-colour layer (Green from RGB) since the red tissue slices were clearly darker than the white background in this layer.

(1) *Pre-processing*: An artefact from the imaging procedure was that the images were slightly darker towards the edges than in the centre. To adjust for this, a shading correction (Gonzalez and Woods, 2008) was used (1) for all pixels (x, y), where f_1 is the corrected image, f_0 is the original G-layer image and f_{blank} is the G-layer from an image without salmon slices, i.e. a blank sheet:

$$f_1(x, y) = f_0(x, y)/f_{\text{blank}}(x, y) \quad (1)$$

for all pixels (x, y) in f_0 and f_{blank}. The image f_1 was then median filtered by a 3×3-mask (T) to remove any minor noise (Gonzalez and Woods, 2008) (Fig. 4):

$$f_2 = T(f_1) = \text{medfilt2}(f1, [3\,3]), \quad (2)$$

where 'medfilt2' is a function in the MATLAB Image Processing Toolbox.

(2) *Segmentation from background*: The Otsu thresholding method (Chi et al., 1996; Otsu, 1979) was then used on the median filtered image f_2 to find the threshold (T) between the light pixels of the background and the dark pixels of the slices (Fig. 4) to create a black and white (binary) image $\alpha(x, y)$ (Fig. 5):

$$\alpha(x, y) = \begin{cases} 1 \text{ if } f_2(x, y) < T = \text{graythresh}(f_2) \\ 0 \text{ otherwise} \end{cases}, \quad (3)$$

for all pixels (x, y) in f_2, and where 'graythresh' is a function in the MATLAB Image Processing Toolbox. The 'graythresh' function automatically finds the global image threshold using Otsu's method.

(3) *Labelling of each slice*: Each slice (four slices in each image) was then assigned a unique label in accordance to the location in the image (function bwlabel, Matlab). The output of this operation is an array of the same size as an input array, containing labels for

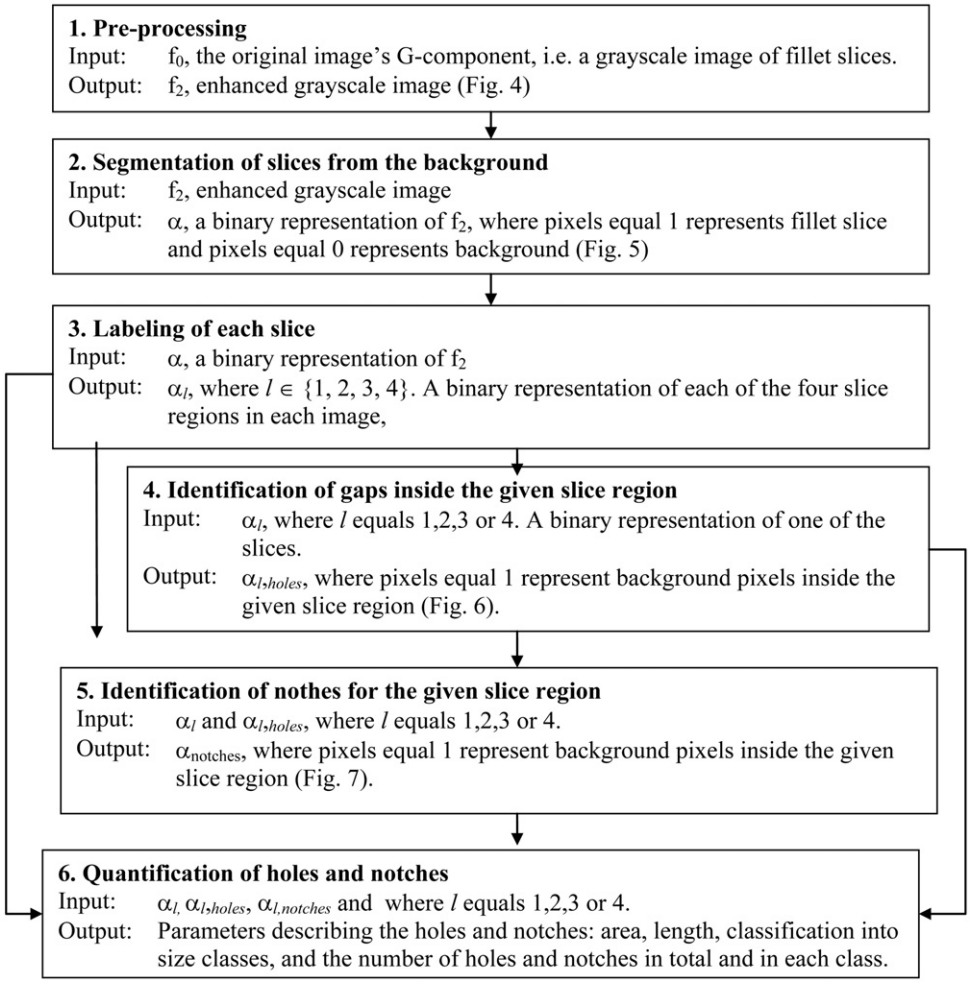

Fig. 3. Flowchart: segmentation and quantification of gaps and notches.

the connected objects in α. The result is an image α where the pixels (x, y) of the background have a label value of 0, and the four slices labels from 1 to 4. The next set of operations was performed on each slice individually; $\alpha_l = \alpha$ equals 1, where $l \in \{1, 2, 3, 4\}$.

(4) *Identification of gaps inside the given slice region*: The gaps in the respective slice were identified by first inverting the labelled segmentation image α_l, and then performing a labelling operation (function bwlabel, Matlab) (Fig. 6). The region labelled 1 in $\neg\alpha_l$ is by design the background; regions with higher labels are gaps ($\alpha_{\text{holes}} = \neg\alpha_l > 0$). The area of gaps was the sum of the area of individual gaps (function regionprops, Matlab).

(5) *Identification of notches*: The notches were identified by filling out the gaps in the border of the given slice region (morphological closing; Gonzalez and Woods, 2008) and then subtracting the slice region, to preserve only the notches. First a binary slice image without holes $\alpha_{l,0} = \alpha_l \vee \alpha_{1,\text{holes}}$ were created. A morphological closing operation (dilation followed by erosion; Glasbey and Horgan, 1995) was then performed on this using the Euclidean distance transform (Borgefors, 1986; Gonzalez and Woods, 2008) and a distance threshold of 60 (Fig. 7):

$$\begin{aligned} \alpha_{1,1} &= \text{bwdist}(\alpha_{1,0}) < 60 \quad \text{dilation operation} \\ \alpha_{1,2} &= \neg(\text{bwdist}(\neg\alpha_{1,1}) < 60 + 2) \quad \text{erosion operation} \end{aligned} \tag{4}$$

where bwdist is a function in the MATLAB Image Processing Toolbox. The notches in the border were then identified as the difference between the slice region with a smoothed border and the original slice region (Fig. 7):

$$\alpha_{l,\text{notches}} = \alpha_{l,0} \wedge \neg\alpha_{l,2} \tag{5}$$

(6) *Quantification of holes and notches*: The identified gaping regions were quantified according to number and size and according to modified Andersen scale (Andersen et al., 1994; Table 1) grading the holes by area and notches by length (regionprops, Matlab). Perforations with area between 1 mm^2 and 25 mm^2 were defined as

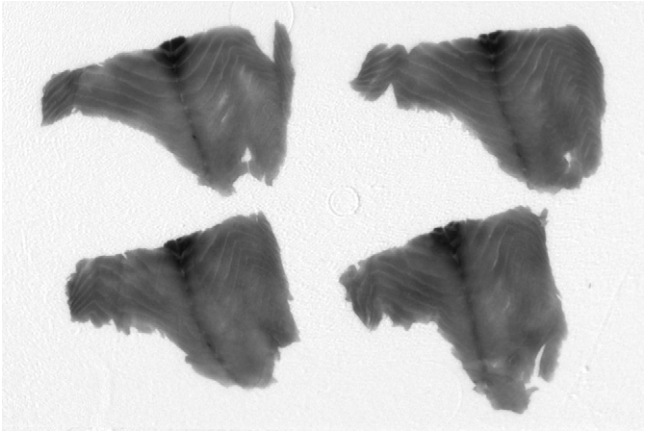

Fig. 4. The G-layer of the RGB image in Fig. 2 after preprocessing.

Fig. 5. Segmentation of each slice on the image (automated image analysis).

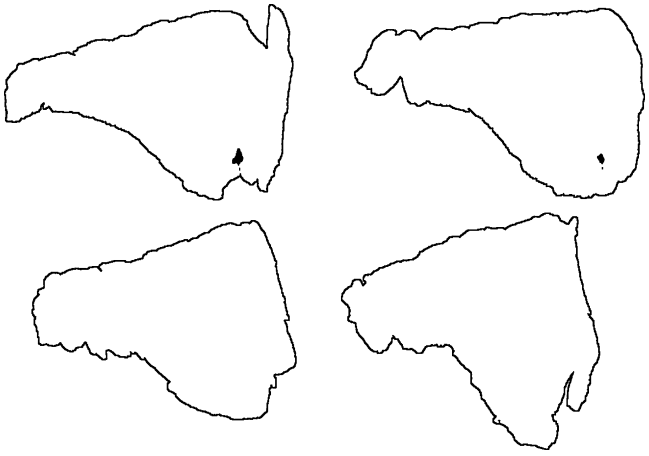

Fig. 6. Segmentation of gaps (black area on the image) (automated image analysis). The borders of the slice regions are given for convenience.

Table 1
Modified Andersen scale (Andersen et al., 1994) used to classify smoked slices according to gaping severity.

Score	Description
0	No gaping
1	Few small[a] slits (less than 5)
2	Some small slits (less than 10)
3	Many slits (more than 9 small or a few (less than 5) large[b]
4	Severe gaping (many large slits (less than 10 large slits))
5	Extreme gaping (the fillet slice falls apart (more than 9 large slits)

[a] <4.5 mm (length threshold) or <25 mm^2 (area threshold).
[b] >4.5 mm (length threshold) or >25 mm^2 (area threshold).

'small gaps', whereas those >25 mm^2 were 'big gaps'. Notches in the border were categorised in accordance to the main axis length as 'small' (1–25 mm) and 'big' (>25 mm).

All these operation (Fig. 3) are assembled as one computer script (programme) and are executed consequently and automatically.

2.4. Manual image analysis method for gaping evaluation

Manual image analysis by three independent assessors was performed on all images (77) taken into automatic analysis. The

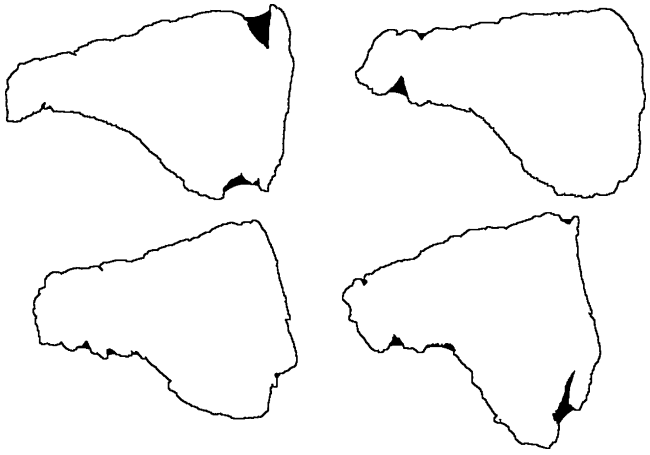

Fig. 7. Segmentation of notches (black areas on the image) (automated image analysis). The borders of the slice regions are given for convenience.

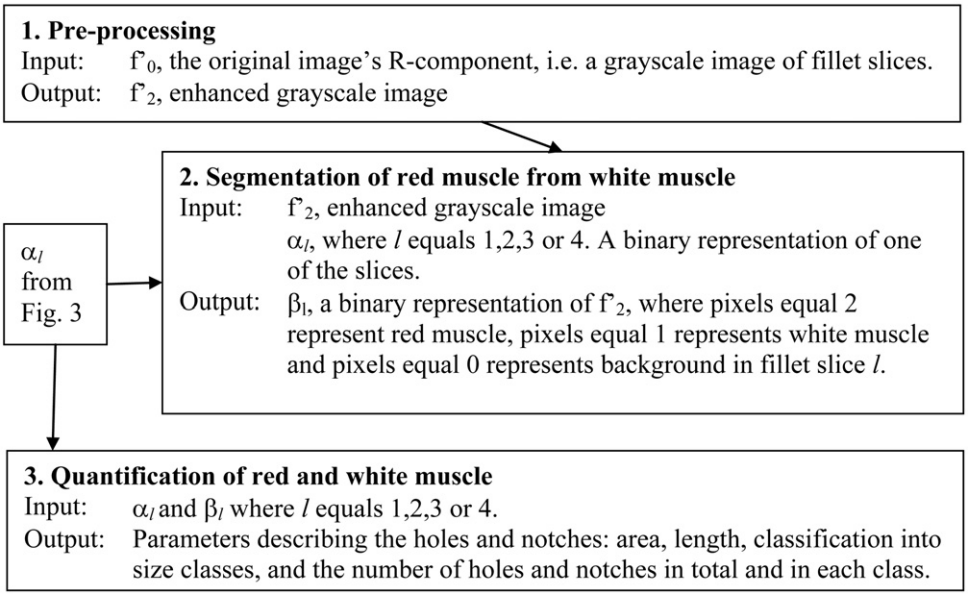

Fig. 8. Flowchart: segmentation and quantification of red muscle from white muscle.

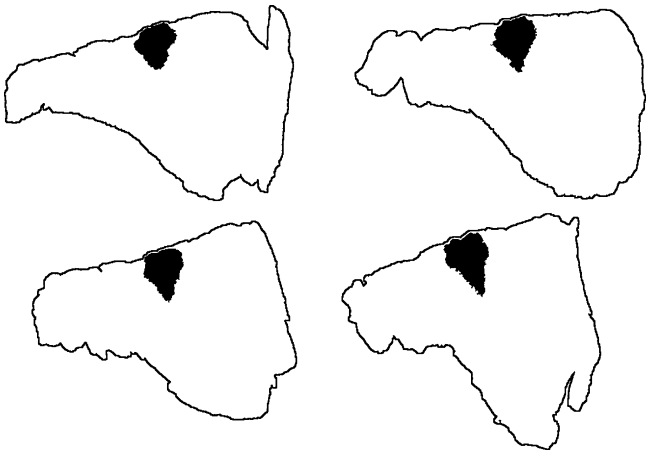

Fig. 9. Segmentation of red muscle area (black on the image) (automated image analysis).

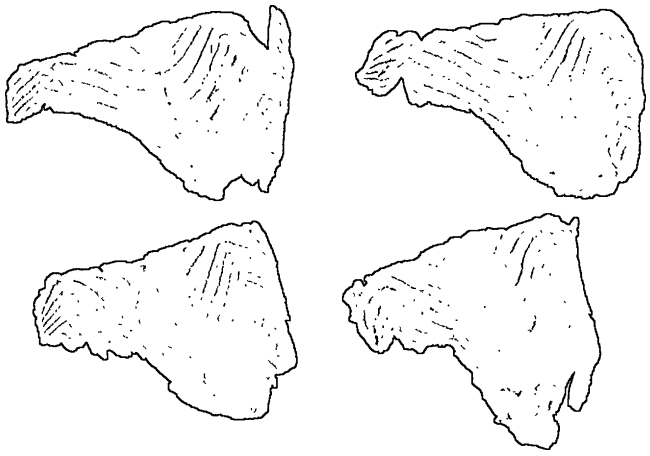

Fig. 10. Segmentation myocommata (black area on the image) (automated image analysis).

identified gaping regions were quantified as described above. In addition, the estimation of co-localisation of gaping between red and white muscle types was done. The median results of manual assessment were compared to automatic image analysis.

2.5. Automatic image analysis of slice shape

The shapes of the individual slices were quantified by morphological features (function regionprops, Matlab), including area, perimeter, compactness, roundness, convexity and eccentricity (Table 2) (Glasbey and Horgan, 1995).

2.6. Automatic image analysis of red and white muscle

The red muscle had a clearly darker shade than the white muscle in the R-layer of the RGB-images. To segment the red muscle from the white muscle, the same shading correction, median filtering, the Otsu thresholding method and labelling was done as described above (step 1 and 2, Fig. 3), but for the R-layer instead of the G-layer and only for the pixels representing fillet slice (Fig. 8). The area and maximum axis length of red muscle region was evaluated for each slice by the use of segmented red muscle image (Fig. 9). All these operation (Fig. 8) are assembled as one computer script (programme) and fully automatic.

In addition the evaluation of gap distribution in red and white muscle types was performed by the mean of automated image analysis.

2.7. Automatic image analysis of myocommata

The white myocommata stripes were segmented from the white muscle region (Fig. 10) as described by Stien et al. (2007). Simply put: for each pixel (x, y) in the white muscle region the image analysis tests if the given pixel is substantially lighter than its horizontal or vertical neighbours:

$$\beta(x,y) = \begin{cases} 1 \text{ if } f_3(x,y) > \dfrac{1}{11}\displaystyle\sum_{i=-5}^{5}(x+i,y) + 0.05 \cdot \mathrm{m} \\ 1 \text{ if } f_3(x,y) > \dfrac{1}{11}\displaystyle\sum_{i=-5}^{5}(x,y+i) + 0.05 \cdot \mathrm{m} \\ 0 \text{ otherwise} \end{cases} \quad (6)$$

where m is the mean value for the white muscle region.

All these operation are assembled as one computer script (programme) and are executed consequently and automatically.

2.8. Validation and statistical analysis

The results from the automatic segmentation of gaps, red muscle and myosepts were compared with the results from the visual inspection performed by an expert (Hoogs and Collins, 2007; Le et al., 2008; Schmid, 1999). Statistical analysis was performed using the MATLAB® Statistics Toolbox (Version 7.10.0499 (R2010a), 32-bit (win 32) and the R computer language (R Development Team, 2011). A nonparametric Spearman's rank correlation test (function corr, Matlab) was used to evaluate correlation between variables (Crawley, 2007). Wilcoxon rank sum test (Crawley, 2007) was performed to evaluate difference in size and in myocommata area for slices with and without gaps.

3. Results

3.1. Comparing automatic with manual assessment of gaping

The average number of small and big gaps per slice (mean (SE)) was 1.3 (0.1) and 0.4 (0.04) for automatic and 1.2 (0.09) and 0.3 (0.04) for manual image analysis, whereas the average number of small and big notches per slice was 5.0 (0.15) and 0.1 (0.02) for automatic and 2.1 (0.1) and 0.1 (0.02) for manual image analysis. There were positive correlations between the automatic and the manual enumeration of small ($r = 0.80$, p-value < 0.05) and big ($r = 0.82$, p-value < 0.05) gaps as well as small ($r = 0.63$, p-value < 0.05) and big ($r = 0.66$, p-value < 0.05) notches in the slice borders. In accordance with the Andersen scale adopted for evaluation of gaping in slices (Table 1) there was a correlation for manually and image analysis determined gap occurrence (Fig. 11, $r = 0.83$, p-value < 0.05) as well as for manual and image analysis derived data on notches (Fig. 11; $r = 0.54$, p-value < 0.05).

3.2. Slice area parameters in relation to gaping

There was found a strong negative correlation between convexity (Table 2) and notches area in slices ($r = -0.84$, p-value < 0.05). There was found a weak but significant correlation between notches and gap numbers ($r = 0.35$, p-value < 0.05).

A developed algorithm applied for segmentation of the area of red muscle in the slice resulted in correctly segmented red muscle area in 94.8% of samples and confirmed by subsequent expert visual assessment (Hoogs and Collins, 2007; Le et al., 2008; Schmid, 1999). The red muscle area was 8.34 (0.15) cm^2 and it comprised 6.5% of the whole slice area of was 128.4 (0.91) cm^2. No gaps were found in red muscle areas of slices, only in the white muscle,

Table 2
Measures of slice shape.

Measure	Formulae	Description (Glasbey and Horgan, 1995)	Mean (SE)
Compactness	$4\pi \frac{\text{area}}{(\text{perimeter})^2}$	The ratio of the area of an object to the area of a circle with the same perimeter	0.49 (0.01)
Roundness	$4\pi \frac{\text{area}}{(\text{convex perimeter})^2}$	The ratio of the area of an object to the area of a circle with the same convex perimeter	0.63 (0.01)
Convexity	$\frac{\text{convex hull perimeter}}{\text{perimeter}}$	The ratio of the convex hull perimeter and the object's perimeter	0.88 (0.01)
Eccentricity	$\frac{\text{length}}{\text{width}}$	The ratio of the length of an object's main inertia axis (length) to the length of an object's minor inertia axis (width)	0.79 (0.01)

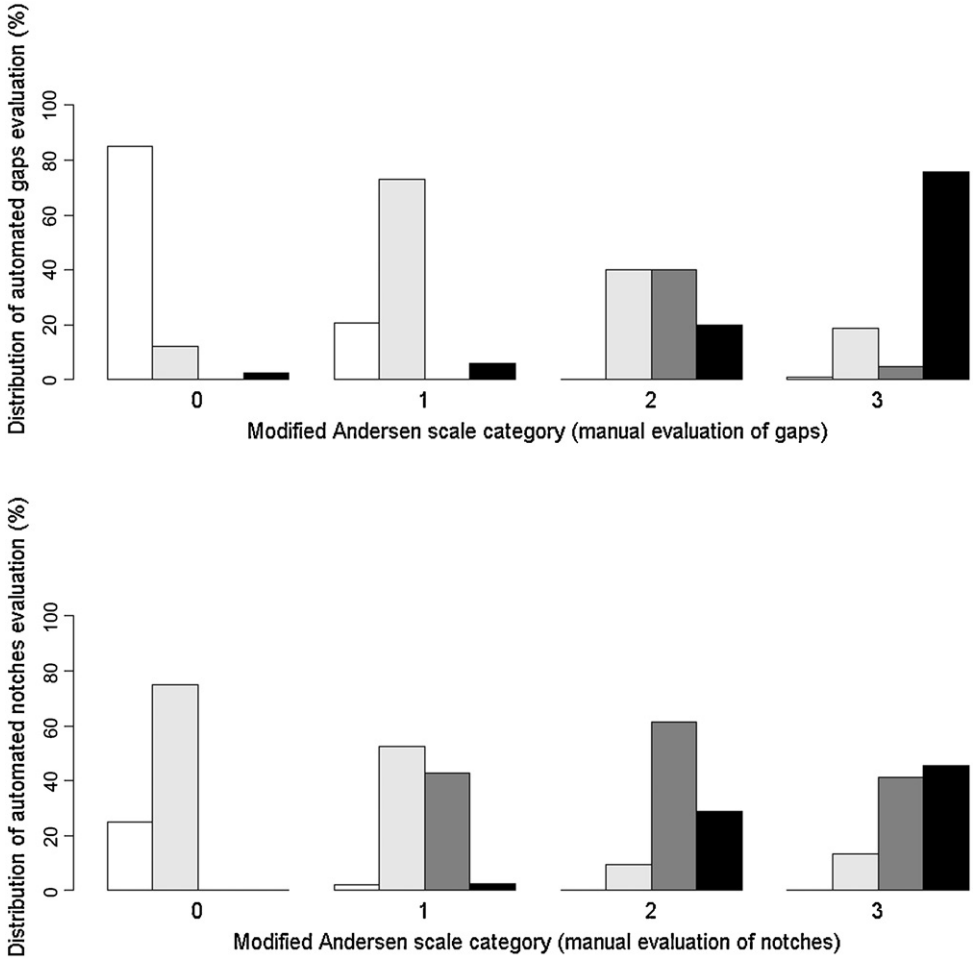

Fig. 11. Manual vs automatic assesment of gaping using the modified Andersen scale (Table 1) in salmon slices ($n = 308$); bar explanations in modified Andersen scale white bar = 0, light-gray bar = 1, dark-gray bar = 2, black bar = 3 in modified Andersen scale. A) Gaps (top); B) Notches (bottom).

evaluated either with automated image analysis or manually. In spite of the finding that the total area of slices without any gaps was significantly smaller (p-value < 0.05; Table 3) than area of slices with gaps, the myocommata area of intact slices was significantly bigger (p-value < 0.05; Table 3) than the myocommata area of slices with gaps. Meanwhile the degree of gaping did not correlate significantly with myocommata area ($r = -0.02$, $p = 0.7$). Moreover, there was very weak but significant negative correlation between area of white stripes and slice area (cor = −0.2643361, p-value < 0.001), while the degree of gaping correlated positively with slice area ($r = 0.29$, $p < 0.001$).

Table 3
Measures of slice shape.

Parameter	Slices without gaps	Slices with gaps
Slice numbers	98	210
Area of slice (mean (SE))	121.26 (1.65) cm^2	131.73 (1.03) cm^2
Area of myosepts (mean (SE))	2.88 (0.16) cm^2	2.57 (0.10) cm^2

4. Discussion

In the current study there was a high correlation between the manual analysis and automatic evaluation of gap number. A less profound correlation was demonstrated between the results of automatic and manual evaluation of notches and can be explained by the relative difficulty in manual quantification of small notches. The human vision is excellent at qualitative task (Glasbey and Horgan, 1995). Meanwhile computer is better for extracting quantitative information from images, because in this case, it is no need to rely on the opinions of several experts and it is consistent

from day to day (Glasbey and Horgan, 1995). This means that the objective image analysis is more reliable than manual analysis and hence more suitable for gap recognition.

Traditional scales for gaping evaluation in fillets (Andersen et al., 1994; Espe et al., 2004b; Kiessling et al., 2004) are hardly suitable for fillet slices because of their size difference. Nonetheless, the Andersen scale (Andersen et al., 1994) provided useful semi-quantitative categories (Table 1) which matched well with the manual and automated evaluation of gaps (Fig. 11) and notches (Fig. 11). However the lack of quantitative sensitivity of Andersen scale could mask the profound differences in numbers of gaps and notches between slices. The total gap/notch count is more sensitive than the interval based Andersen scale and hence the computer evaluation of total gap count is more suitable for gaping evaluation.

Morphological parameters (Glasbey and Horgan, 1995) such as eccentricity, convexity, compactness and roundness represent variations in slice shape (Table 2). Moreover, we have found that notches can be described by the morphological parameter convexity (Table 2). A weak correlation between number of notches and gaps in slices was determined in the present study. The existence of such correlation is reasonable, because both characteristics are associated with reduction of muscle integrity.

Variation in fillet processing can lead to the production of salmon slices with unnecessarily large proportions of red muscle tissue and consequently a downgrading of the product due to the brownish colour and taste of red muscle. The algorithm (Fig. 8) successfully detected the red muscle area (Fig. 9), and no gaps were found in this tissue. While not conclusive, because of difference in the size of white and red muscle, this suggests a link between muscle type and resistance to gaping. This may be due to the physical characteristics of red muscle, with narrower myofibers (Kiessling et al., 2006) and a different association with connective tissue than has white muscle. Moreover fish pre-slaughter activity (Merkin et al., 2010) associated with anaerobic glycolysis (Poli et al., 2005) might stimulate gaping development in white muscle post-mortem.

Myocommata can be visualised (Fig. 10) and evaluated using our algorithm. This connective tissue appears as white stripes in the red salmon slice and can negatively affect the perception of slice colour.

In this study slices with no gaping had significantly more myocommata per unit muscle than slices with gaps. This is not surprising taking into account the known co-occurrence of gaping and big fillet areas without clear separation between the myotome-myocommata (soft band). Anecdotal evidence from the Norwegian fish farming industry in 2007 told of a high co-occurrence of large gaps and prominent jelly-like band in the salmon fillet (Erikson et al., 2012; Martinez et al., 2011). However in the present study smaller slices were less affected by gaping and had relatively more connective tissue. Gaping and myosept integrity can be independently associated with slice size.

The described algorithms could be efficiently used in the fish processing industry in high speed assessment of sliced fillets. Moreover, the results demonstrate the potential of using automatic image analysis for the quantification of fish slice/fillet characteristics associated with gaping and hence the investigation of the gaping phenomenon itself.

5. Conclusions

The developed automatic image analysis algorithms offer a good possibility for quantification and qualification of gaps as well as other morphological parameters in fillet slices. Gaps are located specifically in the white muscle area. Further to that automatic image analysis can be efficiently used for quantification of fish slice/fillet characteristics connected to gaping. These results demonstrate that image analysis methods can be useful in salmon product processing.

Acknowledgements

The statistical treatment in the present project was a part of SalmoConnect project, granted by Norwegian research council (project number 190485). I want to thank Marine Harvest for help in this project. Special thanks to Sylvie Le Gall and Maryline Paul for their help at Marine Harvest Kritsen fish processing factory. In addition I want to thank Erik Hanson for an amazing teaching course in digital image processing and Gleb Brednikov for long discussions about the mathematical background of image processing.

References

Andersen, U.B., Strømsnes, A.N., Steinsholt, K., Thomassen, M.S., 1994. Fillet gaping in farmed Atlantic salmon (*Salmo salar*). Norwegian Journal of Agricultural Sciences 8, 165–179.

Ashton, T.J., Michie, I., Johnston, I.A., 2010. A novel tensile test method to assess texture and gaping in salmon fillets. Journal of Food Science 75, S182–S190, http://dx.doi.org/10.1111/j.1750-3841.2010.01586.x.

Balaban, M.O., Sengor, G.F.U., Soriano, M.G., Ruiz, E.G., 2011. Quantification of gaping, bruising, and blood spots in salmon fillets using image analysis. Journal of Food Science 76, E291–E297, http://dx.doi.org/10.1111/j.1750-3841.2011.02060.x.

Bernardi, C., Ripamonti, B., Campagnoli, A., Stella, S., Cattaneo, P., 2009. Shelf-life of vacuum packed Alaskan, Scottish and Norwegian cold-smoked salmon available on the Italian market. International Journal of Food Science and Technology 44, 2538–2546, http://dx.doi.org/10.1111/j.1365-2621.2009.02081.x.

Birkeland, S., Rora, A.M.B., Skara, T., Bjerkeng, B., 2004. Effects of cold smoking procedures and raw material characteristics on product yield and quality parameters of cold smoked Atlantic salmon (*Salmo salar* L.) fillets. Food Research International 37, 273–286, http://dx.doi.org/10.1016/j.foodres.2003.12.004.

Borgefors, G., 1986. Distance transformations in digital images. Computer Vision Graphics and Image Processing 34, 344–371, http://dx.doi.org/10.1016/s0734-189x(86)80047-0.

Chi, Z., Yan, H., Phạm, T., 1996. Fuzzy algorithms: with applications to image processing and pattern recognition (advances in Fuzzy systems, applications and theory, Vol. 10), World Scientific Pub Co. Pte. Ltd, Singapore. pp. 57–61.

Crawley, M.J., 2007. The R Book. Wiley, Chichester, England; Hoboken, N.J.

Erikson, U., Standal, I.B., Aursand, I.G., Veliyulin, E., Aursand, M., 2012. Use of NMR in fish processing optimization: a review of recent progress. Magnetic Resonance in Chemistry 50, 471–480.

Espe, M., Kiessling, A., Lunestad, B.T., Torrissen, O.J., Rora, A.M.B., 2004a. Quality of cold smoked salmon collected in one French hypermarket during a period of 1 year. Lebensmittel-Wissenschaft Und-Technologie-Food Science and Technology 37, 627–638, http://dx.doi.org/10.1016/j.lwt.2004.01.008.

Espe, M., Ruohonen, K., Bjornevik, M., Froyland, L., Nortvedt, R., Kiessling, A., 2004b. Interactions between ice storage time, collagen composition, gaping and textural properties in fanned salmon muscle harvested at different times of the year. Aquaculture 240, 489–504, http://dx.doi.org/10.1016/j.aquaculture.2004.04.023.

Glasbey, G.A., Horgan, G.W., 1995. Image Analysis for the Biological Sciences. John Wiley & Sons, New York.

Gonzalez, R.C., Woods, R.E., 2008. Digital Image Processing, 3rd ed. Prentice-Hall, Inc., NJ.

Hoogs, A., Collins, R., 2007. Object boundary detection in images using a semantic ontology. In: Proceeedings Twenty-First National Conference on Artificial Intelligence (AAAI-06). Eighteenth Innovative Applications of Artificial Intelligence Conference (IAAI-06), pp. 956–963.

Kiessling, A., Espe, M., Ruohonen, K., Morkore, T., 2004. Texture, gaping and colour of fresh and frozen Atlantic salmon flesh as affected by pre-slaughter iso-eugenol or CO2 anaesthesia. Aquaculture 236, 645–657.

Kiessling, A., Ruohonen, K., Bjørnevik, M., 2006. Muscle fibre growth and quality in fish. Archiv Tierzucht 49, 137–146.

Lavety, J., Afolabi, O.A., Love, R.M., 1988. The connective tissues of fish.9. Gaping in farmed species. International Journal of Food Science and Technology 23, 23–30.

Le, T.V., Kulikowski, C.A., Muchnik, I.B., 2008. A graph-based approach for image segmentation. Advances in Visual Computing. In: Proceedings 4th International Symposium, ISVC 2008, pp. 278–287, http://dx.doi.org/10.1007/978-3-540-89639-5_27.

Martinez, I., Wang, P.A., Slizyte, R., Jorge, A., Dahle, S.W., Canas, B., Yamashita, M., Olsen, R.L., Erikson, U., 2011. Protein expression and enzymatic activities in normal and soft textured Atlantic salmon (*Salmo salar*) muscle. Food Chemistry 126, 140–148.

Merkin, G.V., Roth, B., Gjerstad, C., Dahl-Paulsen, E., Nortvedt, R., 2010. Effect of pre-slaughter procedures on stress responses and some quality parameters in sea-farmed rainbow trout (*Oncorhynchus mykiss*). Aquaculture 309, 231–235, http://dx.doi.org/10.1016/j.aquaculture.2010.08.025.

Michie, 2001. Causes of downgrading in the salmon farming industry. In: Kestin, S.C., Warriss, P.D. (Eds.), Farmed Fish Quality. John Wiley & Sons, Oxford, UK, p. 129–136.

Misimi, E., Mathiassen, J.R., Erikson, U., 2007. Computer vision-based sorting of Atlantic salmon (*Salmo salar*) fillets according to their color level. Journal of Food Science 72, S30–S35, http://dx.doi.org/10.1111/j.1750-3841.2006.00241.x.

Otsu, N., 1979. Threshold selection method from gray-level histograms. IEEE Transactions on Systems Man and Cybernetics 9, 62–66.

Poli, B.M., Parisi, G., Scappini, F., Zampacavallo, G., 2005. Fish welfare and quality as affected by pre-slaughter and slaughter management. Aquaculture International 13, 29–49.

Quevedo, R.A., Aguilera, J.M., Pedreschi, F., 2010. Color of salmon fillets by computer vision and sensory panel. Food and Bioprocess Technology 3, 637–643, http://dx.doi.org/10.1007/s11947-008-0106-6.

R Development Team, 2011. R: A Language and Environment for Statistical Computing. R Foundation for Statistical Computing, Vienna, Austria.

Rasmussen, R.S., 2001. Quality of farmed salmonids with emphasis on proximate composition, yield and sensory characteristics. Aquaculture Research 32, 767–786.

Robb, D.H.F., 2001. The relationship between killing methods and quality. In: Kestin, S.C., Warriss, P.D. (Eds.), Farmed Fish Quality. Fishing News Books, Cornwall, pp. 220–233.

Roth, B., Birkeland, S., Oyarzun, F., 2009. Stunning, pre slaughter and filleting conditions of Atlantic salmon and subsequent effect on flesh quality on fresh and smoked fillets. Aquaculture 289, 350–356.

Schmid, P., 1999. Segmentation of digitized dermatoscopic images by two-dimensional color clustering. IEEE Transactions on Medical Imaging 18, 164–171.

Stien, L.H., Kiessling, A., Marine, F., 2007. Rapid estimation of fat content in salmon fillets by colour image analysis. Journal of Food Composition and Analysis 20, 73–79, http://dx.doi.org/10.1016/j.jfca.2006.07.007.

Stien, L.H., Manne, F., Ruohonene, K., Kause, A., Rungruangsak-Torrissen, K., Kiessling, A., 2006. Automated image analysis as a tool to quantify the colour and composition of rainbow trout (*Oncorhynchus mykiss* W.) cutlets. Aquaculture 261, 695–705, http://dx.doi.org/10.1016/j.aquaculture.2006.08.009.